

Ioannis P. GEROTHANASSIS,<sup>1</sup> Anastassios TROGANIS,<sup>2</sup>  
Vassiliki EXARCHOU,<sup>1</sup> and Klimentini BARBAROSSOU<sup>1</sup>

<sup>1</sup> University of Ioannina, Department of Chemistry

<sup>2</sup> University of Ioannina, Department of Biological Applications and Technologies

## NUCLEAR MAGNETIC RESONANCE (NMR) SPECTROSCOPY: BASIC PRINCIPLES AND PHENOMENA, AND THEIR APPLICATIONS TO CHEMISTRY, BIOLOGY AND MEDICINE

*Received 20 May 2002; in final form 24 May 2002*

**ABSTRACT:** Nuclear Magnetic Resonance (NMR) spectroscopy has made a tremendous impact in many areas of chemistry, biology and medicine. In this report a student-oriented approach is presented, which enhances the ability of students to comprehend the basic concepts of NMR spectroscopy and the NMR spectra of various nuclei. The origin of chemical shifts, coupling constants, spin relaxation and the Nuclear Overhauser Effect (NOE) will be discussed and their relation to molecular structure will be provided. A wide range of applications of NMR spectroscopy is presented, including exchange phenomena, the identification and structural studies of complex biomolecules, such as proteins, applications to food analysis, clinical studies, NMR as a microscope and magnetic tomography. [*Chem. Educ. Res. Pract. Eur.*, 2002, 3, 229-252]

**KEY WORDS:** *NMR spectroscopy; nuclear magnetic moment; screening constant; coupling constant; nuclear Overhauser effect (NOE); nuclear relaxation; applications of NMR*

### INTRODUCTION

Nuclear magnetic resonance (NMR) spectroscopy was discovered shortly after the Second World War, and since then its applications to chemistry have been continuously expanding. It was natural then that NMR took an important part in undergraduate chemistry education, being taught within various courses: physical chemistry, organic, inorganic and analytical chemistry. In recent years, the applications of NMR have been extended to biology and medicine, so they have also become an integral part of courses in these subjects.

The basic principles are usually covered in the physical chemistry course, and now every undergraduate physical chemistry textbook has a chapter on it. In addition, numerous monographs have been written on NMR, but these are usually addressed at the advanced undergraduate and graduate levels (Ernst, Bodenhausen, & Wokaun, 1987). It is also well-known that, conceptually, NMR is a very difficult subject to teach and learn; this is because this subject is grounded on physical concepts of electricity and magnetism and classical mechanics and is further extended with quantum mechanical treatments. It is reasonable, then, that a course in NMR poses considerable learning obstacles for the student.

The purpose of this article is twofold; on the one hand to propose a teaching sequence for undergraduate student in various disciplines that, in our opinion, is conceptually sound; on the other hand, to emphasize and describe selected (both traditional and modern)

applications of NMR to chemical structure determination, (in solution and in the solid state), food analysis, clinical investigations, and NMR microscopy and imaging.

## OVERVIEW OF THE CONCEPTS

### The nuclear magnetic moment

Any motion of a charged particle has an associated magnetic field. This means, that a magnetic dipole is created, just like an electrical current in a loop creates a magnetic dipole, which in a magnetic field corresponds to a magnetic moment  $\mu$  (Figure 1). The magnetic moment  $\mu$  of a nucleus is intimately connected with its spin angular momentum. To be more precise  $\mu$  is proportional to  $I$ , which is the angular momentum quantum number usually called the nuclear spin, with a proportionality constant  $\gamma$  known as gyromagnetic ratio:

$$\mu = \gamma I \quad (1)$$

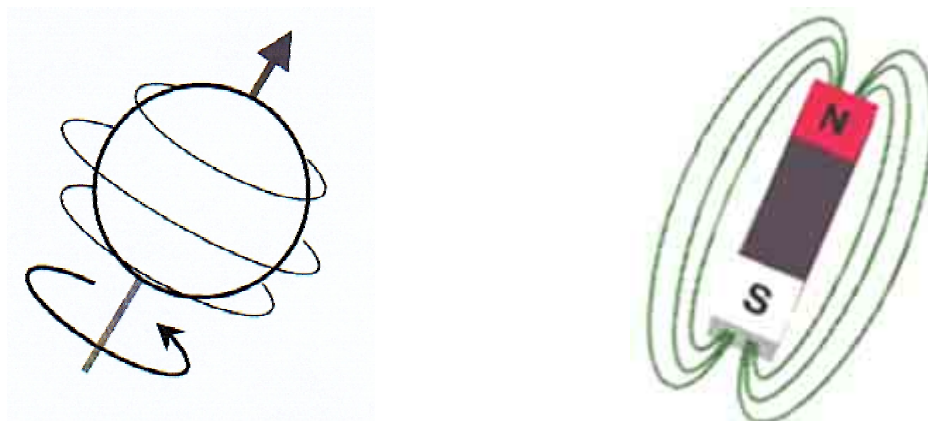


FIGURE 1. A spinning nucleus can be regarded as a microscopic magnet.

### Larmor precession

Let us consider the classical motion of a magnetic moment,  $\mu$ , in a uniform externally applied strong magnetic field  $\mathbf{B}_0$  under the condition of constant total energy. The movement of  $\mu$  traces out a cone about  $\mathbf{B}_0$ , which is analogous to the motion of a gyroscope running in friction-free bearings under the influence of the Earth's field (Figure 2). Such motion is referred to in general as Larmor precession. The precession frequency,  $\nu_0$ , is given by:

$$\nu_0 = |\gamma| \mathbf{B}_0 / 2\pi \quad (2)$$

Suppose there is an additional externally applied, but weak magnetic field,  $\mathbf{B}_1$ , perpendicular to  $\mathbf{B}_0$ . Such a field will also exert a torque on  $\mu$ , tending to change the angle  $\theta$  between  $\mu$  and  $\mathbf{B}_0$ . However, if  $\mathbf{B}_1$  is fixed in direction and magnitude, it will alternately try to increase and decrease  $\theta$  as  $\mu$  precesses. Since  $\mathbf{B}_1$  is stated to be weak, the net effect will be a slight wobbling in the precession of  $\mu$ . Alternatively, the motion of  $\mu$  can be described as caused by a resultant field  $\mathbf{B}_0 + \mathbf{B}_1$ . If, on the other hand,  $\mathbf{B}_1$  is not fixed, but is rotating about  $\mathbf{B}_0$  with the same frequency as the precession of  $\mu$ , its orientation with respect to  $\mu$  will be constant. Suppose this orientation is such, that  $\mathbf{B}_1$  is always perpendicular to the plane containing  $\mathbf{B}_0$  and  $\mu$  as in Figure 3; then the torque exerted on  $\mu$  by  $\mathbf{B}_1$  will always be away from  $\mathbf{B}_0$ .

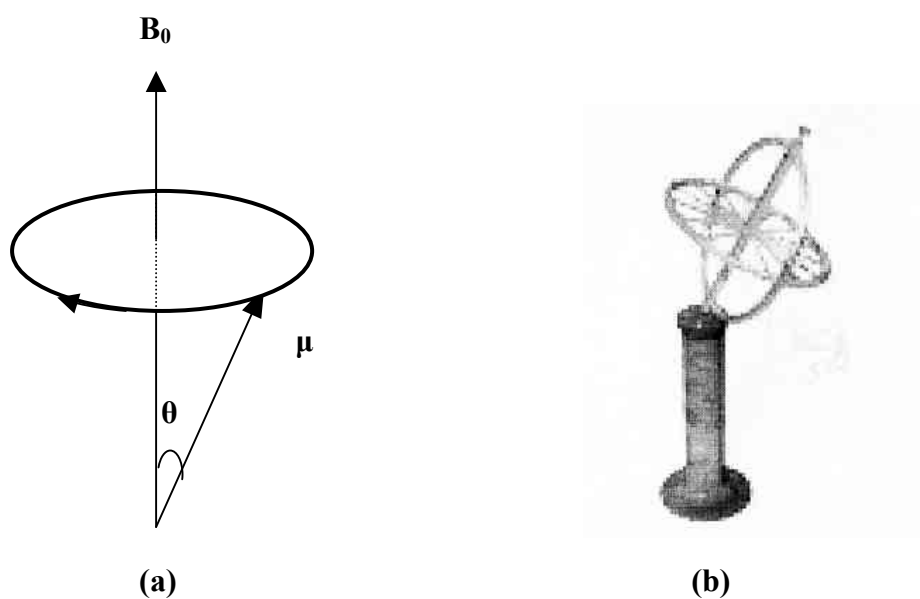


**FIGURE 2.** (a) Precession of a magnetic moment  $\mu$  about an applied magnetic field  $B_0$ . (b) The nuclear precession is analogous to the motion of a gyroscope under the influence of the Earth's field.

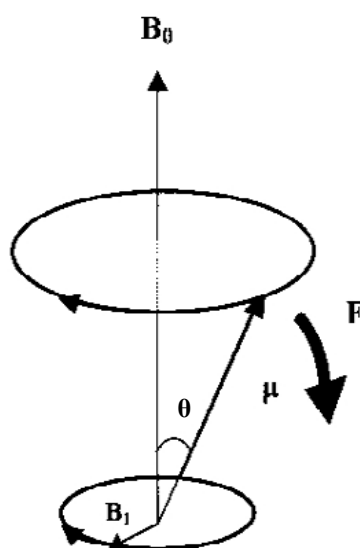


**FIGURE 3.** The effect of a rotating magnetic field,  $B_1$ , on a precessing magnetic moment,  $\mu$ . When  $B_1$  is perpendicular to the  $B_1 - \mu$  plane, there is a force  $F$  acting to increase the angle between  $B_0$  and  $\mu$ . If  $\mu$  and  $B_1$  are rotating at the same rate, this force acts always away from  $B_0$  and therefore has a consistent effect (Harris, 1983).

Consequently, an accumulated effect on  $\mu$  is possible. Since changing  $\theta$  corresponds to changing the energy of  $\mu$  in  $B_0$ , this condition is described as resonance – the frequency,  $\nu$ , of the field  $B_1$  required must equal the Larmor precession frequency of equation. (2) (Harris, 1983). The energy for the change of  $\theta$  is, of course, derived from the rotating field  $B_1$ , which

is supplied by radio frequency electromagnetic radiation.

### Quantum mechanical description

According to the classical picture the atomic nucleus, assumed to be spherical, rotates about an axis and thus, possesses a nuclear or intrinsic angular momentum  $\mathbf{P}$ . Quantum mechanical considerations show that, like many other atomic properties, this angular momentum is quantized:

$$\mathbf{P} = \hbar\sqrt{\mathbf{I}(\mathbf{I} + 1)} \quad (3)$$

where  $\hbar = h/2\pi$ , ( $h$  is Planck's constant). The nuclear spin can have values  $\mathbf{I} = 0, 1/2, 1, 3/2, 2, \dots$  up to 7. As it will be explained below, neither the values of  $\mathbf{I}$  nor those of  $\mathbf{P}$  can yet be predicted from theory.

If a nucleus with angular momentum  $\mathbf{P}$  and magnetic moment  $\boldsymbol{\mu}$  is placed in a static strong magnetic field  $\mathbf{B}_0$ , the angular momentum takes up an orientation such that its component  $\mathbf{P}_z$  along the direction of the field is an integral or half-integral multiple of  $\hbar$ :

$$\mathbf{P}_z = m_l \hbar \quad (4)$$

where  $m_l$  is the magnetic or directional quantum number with values  $m_l = I, I - 1, \dots, -I$ . It can easily be deduced that there are  $(2I + 1)$  different values of  $m_l$ , and consequently an equal number of possible orientations of the angular momentum and magnetic moment in an external magnetic field  $\mathbf{B}_0$ . For  $^1\text{H}$  and  $^{13}\text{C}$  nuclei, which have  $I = 1/2$ , there are two  $m_l$ -values ( $+1/2$  and  $-1/2$ ) (Figure 4). Thus, if these nuclei are immersed in an external magnetic field, they can only be regarded as being effectively lined up with the field ( $m_l = +1/2$ ) or against the field ( $m_l = -1/2$ ). As with compass needles in the Earth's magnetic field, the more favorable energy state is the one corresponding to alignment with the field. The energy difference between the states  $\Delta E$  is found to be proportional to the strength of the applied field  $\mathbf{B}_0$  at the nucleus; actually,  $\Delta E$  is equal to  $\gamma\hbar\mathbf{B}_0$  (Figure 4).

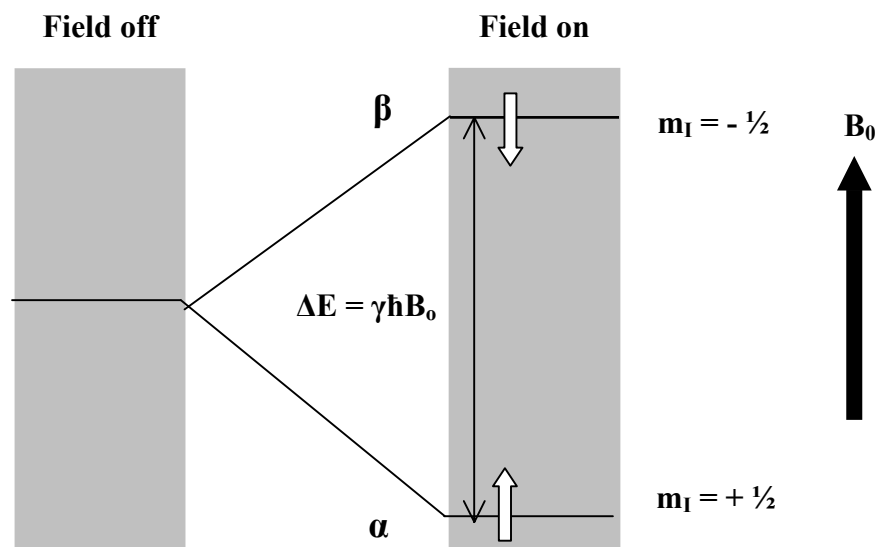


FIGURE 4. The nuclear spin energy levels of a spin- $1/2$  nucleus in a magnetic field (Atkins, 1998).

To observe a nuclear magnetic absorption, we have to adjust either the frequency  $\nu_0$  of the radiation or the strength of the magnetic field at the nucleus,  $\mathbf{B}_0$  until equation (2) holds, i.e. until the point where resonance (energy absorption) occurs.

### What is the nuclear quantum number?

The simplest nucleus is that of hydrogen atom, which consists of one particle only, the proton. The protonic mass ( $1.67 \times 10^{-27}$  kg) and charge ( $+1.60 \times 10^{-19}$  C) are taken as the elementary units of mass and electric charge respectively. Another particle which is a constituent of all nuclei (apart from the hydrogen nucleus) is the neutron; this has unit mass (i.e. equal to that of a proton), no charge and a spin of  $1/2$ . Thus, if a particular nucleus is composed of  $p$  protons and  $n$  neutrons, its total mass is  $p + n$ , its total charge is  $+p$  and its total spin will be a vector combination of  $p + n$  spins, each of magnitude  $1/2$ . The atomic mass is usually specified for each nucleus by writing it as a prefix to the nuclear symbol, e.g.  $^{12}\text{C}$  indicates the nucleus of carbon having an atomic mass of 12. This nucleus contains six protons and six neutrons to make up a mass of 12. The nucleus  $^{13}\text{C}$  (an isotope of carbon) has six protons and seven neutrons.

Each nuclear isotope, being composed of a different number of protons and neutrons will have its own total spin value. Unfortunately, the laws governing the vector addition of nuclear spins are not yet known, so the spin of a particular nucleus cannot be predicted in general (McLauchan, 1972). Deuterium,  $^2\text{H}$ , an isotope of hydrogen containing one proton and one neutron might have a spin of 1 or zero depending on whether the proton and neutron spins are parallel or opposed; it is observed to be 1. The helium nucleus,  $^4\text{He}$ , contains two protons and two neutrons and has zero spin. From these observations the following empirical rules have been formulated:

- (i) Nuclei with both  $p$  and  $n$  even have zero spin (e.g.  $^4\text{He}$ ,  $^{12}\text{C}$ ,  $^{16}\text{O}$ ).
- (ii) Nuclei with both  $p$  and  $n$  odd and mass even, have integral spin [e.g.  $^2\text{H}$ ,  $^{14}\text{N}$  ( $I = 1$ ),  $^{10}\text{B}$  ( $I = 3$ )].
- (iii) Nuclei with odd mass have half-integral spins [e.g.  $^1\text{H}$ ,  $^{15}\text{N}$  ( $I = 1/2$ ),  $^{17}\text{O}$  ( $I = 5/2$ )].

### The ensemble nature of NMR spectroscopy – Population of energy levels

Whenever we measure the ‘spectrum of a molecule’, we actually obtain the response from a very large number of similar molecules contained in some sample cell of size  $\sim 0.5$  mL which may contain as large as  $10^{25}$  spins. Thus far, we have discussed the properties of individual nuclei, but in the following we will investigate how a large number of them distribute themselves between the two energy states available to spin  $-1/2$  particles in an applied field, (McLauchan, 1972). Students, when first confronted with NMR spectroscopy, usually ask: why don’t the nuclear magnetic moments immediately line themselves up in an applied field so that they all occupy the lowest energy state such as in the case of a bar magnet in the earth’s field? The spin magnetic moments orientate themselves in a magnetic field, although they do not all occupy the lowest available energy state. This is a simple consequence of competition between thermal motion and the Boltzmann distribution (Figure 5).

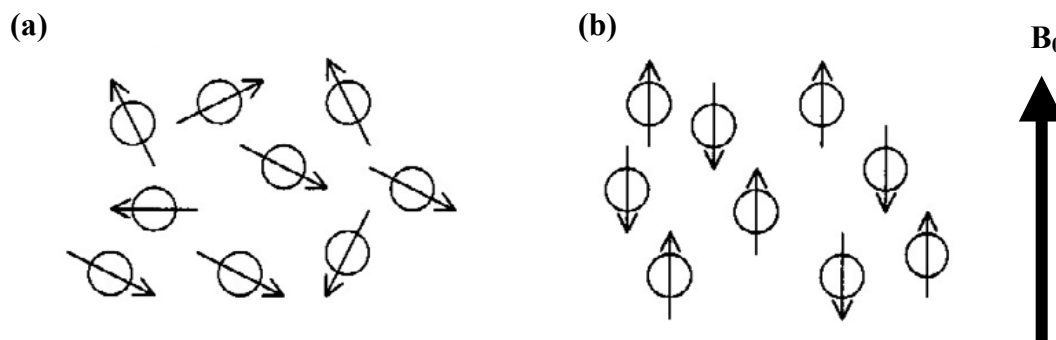


**FIGURE 5.** *The effect of the magnetic field  $B_0$  on the orientation of the spin magnetic moments.*

Providing that the system is in thermal equilibrium with its surroundings, we may calculate the distribution from the Boltzmann law. If  $n_u$  and  $n_l$  are the numbers of particles in the upper and lower levels, respectively, and  $T$  is the absolute temperature, then,

$$\frac{n_u}{n_l} = e^{-\frac{\Delta E}{kT}} \quad (5)$$

where  $k$  is the Boltzmann constant ( $k = 1.38066 \times 10^{-23} \text{ JK}^{-1}$ ) and  $\Delta E$  the energy gap between the two levels (Hore, 1995). Evaluating equation (5) for protons in a field  $B$  of 9.4 Tesla (T), the unit of magnetic field equal to  $1 \text{ kg s}^{-2} \text{ A}^{-2}$ , which is a typical magnetic field strength used for NMR, at a temperature of 300 K, one finds that  $\Delta E = 2.65 \times 10^{-25} \text{ J}$ ,  $kT = 4.14 \times 10^{-21} \text{ J}$  and  $\Delta E/kT = 6.4 \times 10^{-5}$ . Thus, the energy required to reorient the spins is dwarfed by the thermal energy  $kT$ . With such small values of  $\Delta E/kT$ , equation (5) may be simplified using  $e^{-x} \approx 1 - x$ , to obtain the normalized population difference:

$$\frac{n_l - n_u}{n_l + n_u} = \frac{\Delta E}{2kT} \quad (6)$$

With the above numbers, equation (5) gives a population difference of  $3.2 \times 10^{-5}$  or one part in about 31000. This difference will be even smaller for protons in a weaker field, or for nuclei with lower gyromagnetic ratios (i.e. almost all other nuclei of Table 1). The net result of this population difference is an overall magnetization,  $\mathbf{M}_0$ , of the sample in the direction of the  $z$  axis.

In NMR spectroscopy where the upward transitions outnumber the downward transitions by only one in  $10^4$ - $10^6$ , it is as if one detects only one nucleus in every  $10^4$ - $10^6$ . It is therefore of crucial importance to optimize signal strengths, for example by using strong external magnetic fields  $\mathbf{B}_0$  to maximize  $\Delta E$ . Similarly, nuclei with large gyromagnetic ratio and high natural abundance are favoured, hence the popularity of  $^1\text{H}$  as an NMR nucleus.

TABLE 1. Properties of some nuclei with non-zero spin.

Nucleus	Spin	Natural Abundance %	Magnetic moment $\mu^a$	Magnetogyric ratio $\gamma/10^7 \text{ rad T s}^{-1}$	NMR frequency $\nu/\text{MHz}$
$^1\text{H}$	1/2	99.985	2.7927	26.7520	400.000
$^2\text{H}$	1	0.015	0.8574	4.1066	61.402
$^7\text{Li}$	3/2	92.58	3.2560	10.3975	155.454
$^{13}\text{C}$	1/2	1.108	0.7022	6.7283	100.577
$^{14}\text{N}$	1	99.63	0.4036	1.9338	28.894
$^{15}\text{N}$	1/2	0.37	-0.2830	-2.712	40.531
$^{17}\text{O}$	5/2	0.037	-1.8930	-3.6279	54.227
$^{19}\text{F}$	1/2	100	2.6273	25.181	376.308
$^{23}\text{Na}$	3/2	100	2.2161	7.08013	105.805
$^{27}\text{Al}$	5/2	100	3.6385	6.9760	104.229
$^{29}\text{Si}$	1/2	4.70	-0.5548	-5.3188	79.460
$^{31}\text{P}$	1/2	100	1.1305	10.841	161.923
$^{59}\text{Co}$	7/2	100	4.6388	6.317	94.457
$^{77}\text{Se}$	1/2	7.58	0.5333	5.12	76.270
$^{195}\text{Pt}$	1/2	33.8	0.6004	5.768	85.996
$^{199}\text{Hg}$	1/2	16.84	0.4993	4.8154	71.309

<sup>a</sup> magnetic dipole moment in units of the nuclear magneton,  $eh/(4\pi M_p)$ , where  $M_p$  is the mass of the proton.

### The screening constant

In general, a nucleus is not bare but it is surrounded by electrons. Since electrons are moving charges, they obey the laws of electromagnetic induction. So, the applied magnetic field,  $\mathbf{B}_0$ , induces circulation in the electron cloud surrounding the nucleus such that, following Lenz's law, a secondary magnetic field,  $\mathbf{B}'$ , opposed to  $\mathbf{B}_0$ , is produced (Figure 6).

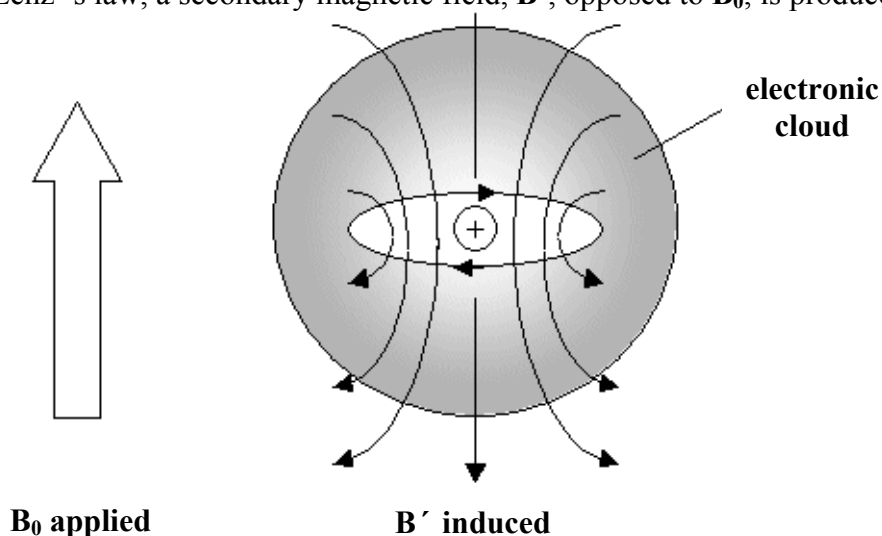


FIGURE 6. An applied magnetic field  $\mathbf{B}_0$  causes the electrons in an atom to circulate within their orbitals. This motion generates an extra field  $\mathbf{B}'$  at the nucleus opposing the  $\mathbf{B}_0$ .

Thus, the local magnetic field that a nucleus experiences, is smaller than the applied field. The nucleus is shielded from the external field by its surrounding electrons by an amount equal to  $\sigma\mathbf{B}_0$  where  $\sigma$  is known as the *shielding or screening constant*, which is a dimensionless quantity (Harris, 1983; Günther, 1995; Gerothanassis & Kalodimos, 1996):

$$\mathbf{B}_{\text{local}} = \mathbf{B}_0(1 - \sigma) \quad (7)$$

This magnetic shielding has the effect that a higher external field is required to meet the resonance condition in an experiment in which the field is varied, while at a constant field,  $\mathbf{B}_0$ , the resonance condition is met at a lower frequency than might be expected.

In a NMR experiment, the inevitable presence of electrons around the nucleus might be thought a disadvantage, since their presence leads to uncertainty as to the precise value of the field experienced by the nucleus under investigation. The electrons are indeed a nuisance if the experiment is only interested in a high precision determination of magnetogyric ratio or in an accurate measurement of the absolute value of a magnetic field by using equation (2). However, for the experiment concerned with the details of the electron density around the nucleus determination of  $\sigma$  might provide a very sensitive method for investigating electronic structure of atoms and molecules, in gases, liquids and solids.

## THE NMR SPECTRA OF VARIOUS NUCLEI

### The case of $^1\text{H}$

The vast majority of molecules of interest to chemists contain hydrogen atoms and, as this nucleus has one of the strongest resonances, it is not surprising that  $^1\text{H}$  NMR has found the widest application. Protons in different chemical groups have different shielding constants, and the resonance condition is satisfied at different  $\nu_0$ .

Let us understand the spectrum of ethanol shown in Figure 7 (Atkins, 1998). The methyl protons form one group; since all the CH bonds are identical and the shielding of each of the nuclei is the same, such nuclei are called magnetically equivalent, and come into resonance at a position governed by their electron density. The two methylene protons are in a different part of the molecule, they therefore have a different electron density and come into resonance at a different frequency. Finally, the proton of the hydroxyl group resonates at yet another value of the applied field. Since we know that oxygen is a much better electron acceptor than carbon (oxygen has greater electronegativity), then the electron density about the hydrogen atom in C-H bonds should be considerably higher than the O-H bonds. We should thus expect  $\sigma_{\text{CH}} > \sigma_{\text{OH}}$  and hence

$$\nu_{\text{CH}} = \gamma\mathbf{B}_0/2\pi (1 - \sigma_{\text{CH}}) < \nu_{\text{OH}} = \gamma\mathbf{B}_0/2\pi (1 - \sigma_{\text{OH}}) \quad (8)$$

Thus, for a given applied field, the CH hydrogen nucleus will precess with a smaller Larmor frequency than that of OH (Banwell, 1994; Atkins, 1998).

Two very important facets of NMR spectroscopy appear in Figure 7:

- (i) Identical nuclei, i.e.  $^1\text{H}$  nuclei, give rise to different absorption positions when in different chemical surroundings. For this reason the separation between absorption peaks is usually referred to as chemical shift.
- (ii) The area of an absorption peak is proportional to the number of equivalent nuclei (i.e. nuclei with the same chemical shift). Note that in the case of ethanol, we can distinguish which group of lines corresponds to which group of protons by their relative intensities.

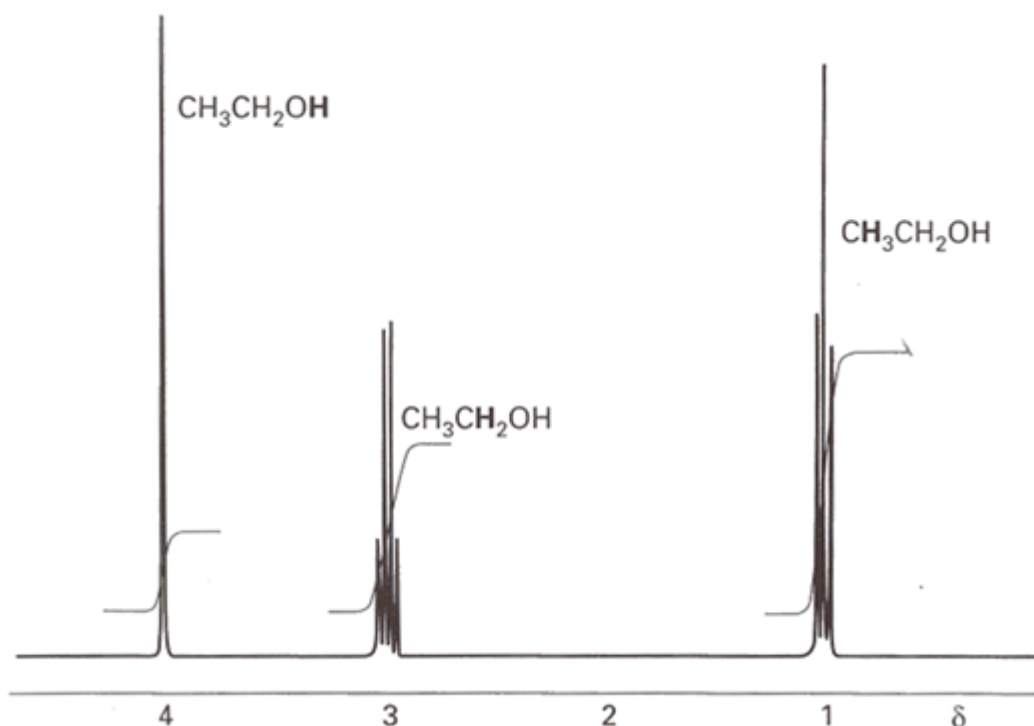


**FIGURE 7.** The  $^1\text{H}$ -NMR spectrum of ethanol. The bold letters denote the protons giving rise to the resonance peak, and the step-like curve is the integrated signal (Atkins, 1998).

The group intensities are in the ratio 3:2:1 because there are 3 methyl protons, 2 methylene protons and 1 hydroxyl proton.

Chemical shift measurements are formally based on the resonance position of the bare proton nucleus as the primary standard. For this there is no shielding, and hence  $\sigma = 0$ . Since this is a quite impracticable standard, the shifts are normally quoted relative to the protons of some standard compound. Tetramethylsilane  $\text{Si}(\text{CH}_3)_4$ , written TMS, which bristles with equivalent protons is a standard frequently chosen.

So, we define the chemical shift in terms of the difference in resonance frequencies between the nucleus of interest (i.e.  $^1\text{H}$ ) and a reference nucleus (i.e.  $^1\text{H}$  of TMS) by means of a dimensionless parameter  $\delta$ . The  $\delta$  values are positive if the sample absorbs to high frequency of the reference absorption at constant field:

$$\delta = 10^6(\nu_{\text{sample}} - \nu_{\text{TMS}})/\nu_{\text{TMS}} \quad (9)$$

Since shielding constants are small, the value  $\nu_{\text{TMS}}$  in the denominator may be replaced by the spectrometer operating frequency  $\nu_0$  or by  $|\gamma|B_0/2\pi$  with little error. Thus,  $\delta$  is related to shielding constants by:

$$\delta = 10^6(\sigma_{\text{TMS}} - \sigma_{\text{sample}}) \quad (10)$$

The factor of  $10^6$  simply scales the numerical value of  $\delta$  to a more convenient size:  $\delta$  values are quoted in *parts per million*, or ppm (Harris, 1983).

Characteristic  $\delta$  chemical shifts of a number of commonly occurring groups are shown in Figure 8.

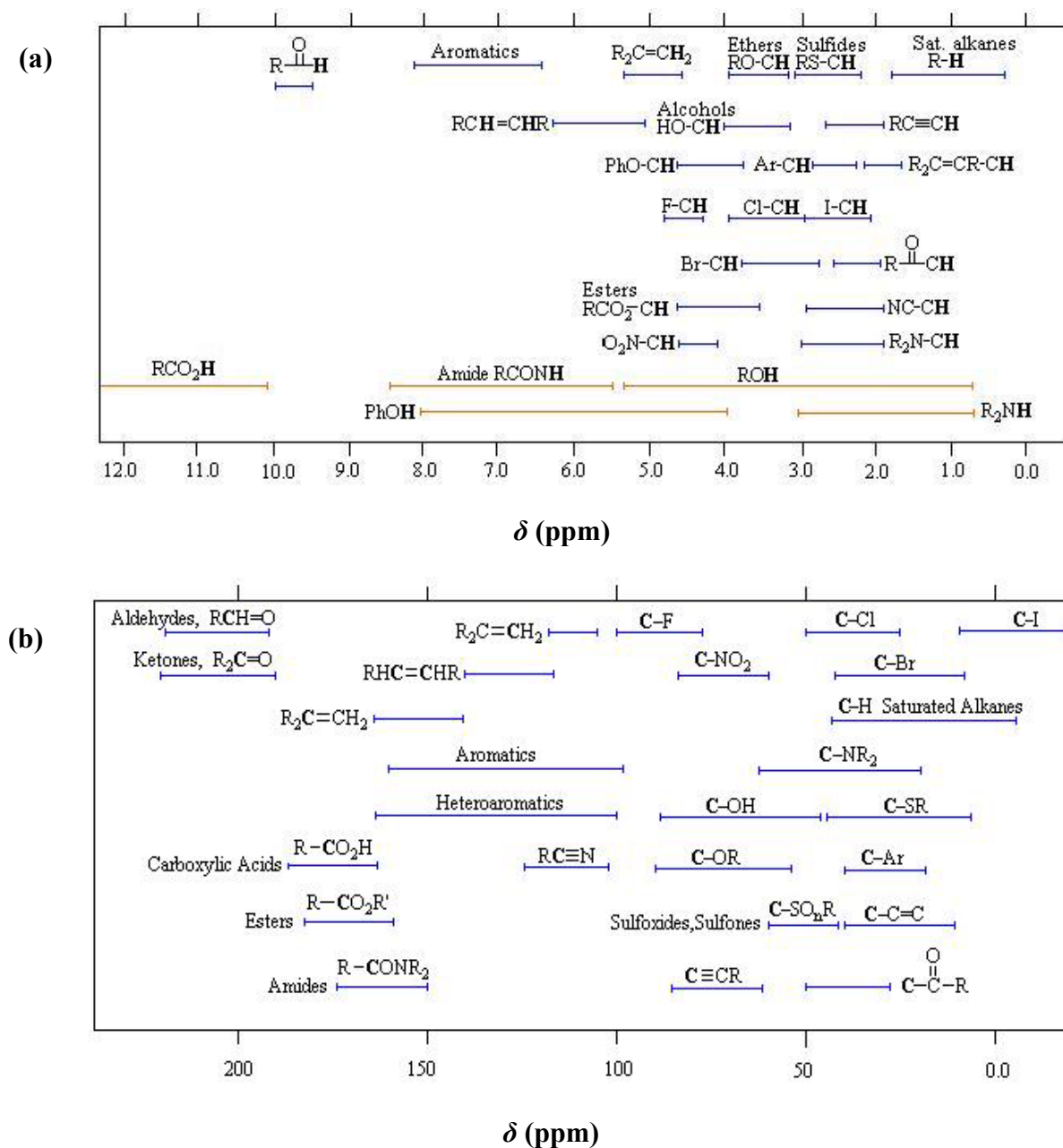


FIGURE 8. The range of typical chemical shifts for (a)  $^1\text{H}$  resonances and (b)  $^{13}\text{C}$  resonances.

### The case of $^{13}\text{C}$

The element carbon consists of the stable isotopes  $^{12}\text{C}$  and  $^{13}\text{C}$  with 98.9 % and 1.1 % natural abundance respectively (Table 1). Only the  $^{13}\text{C}$  nucleus has a magnetic moment with  $I = 1/2$ , while the  $^{12}\text{C}$  nucleus of the major isotope is non-magnetic. Therefore, nuclear magnetic resonance spectroscopy of carbon, which is of great interest for organic chemistry, is limited to the investigation of  $^{13}\text{C}$ . The magnetic moment of the  $^{13}\text{C}$  is smaller than that of the proton by a factor of 4. Consequently,  $^{13}\text{C}$  is less sensitive for the NMR experiment than the proton. Moreover, the low natural abundance renders its detection more difficult and, therefore,  $^{13}\text{C}$  NMR spectroscopy is by far less sensitive than  $^1\text{H}$ -NMR.

The principles governing  $^{13}\text{C}$  chemical shifts are similar to those of  $^1\text{H}$  spectroscopy, although the scale of observed shifts is greater for the former (Figure 8). Chemical shifts of  $^{13}\text{C}$  nuclei are measured (in ppm) from TMS as reference. On  $\delta$  scale,  $^{13}\text{C}$  shifts range from 0 to about 250 ppm. As in proton spectra, the precise chemical shift of a nucleus depends on the atom or atoms attached to it and there are correlations with the electronegativity of substituents. Because of the greater range of chemical shifts,  $^{13}\text{C}$  spectra usually contain a separate resonance for each chemically shifted nucleus in the molecule (very little overlap of resonances occurs) (Banwell, 1994).

### Other heteronuclei

$^{14}\text{N}$ ,  $^{15}\text{N}$ ,  $^{17}\text{O}$ ,  $^{19}\text{F}$  have larger chemical shift ranges than  $^1\text{H}$  and  $^{13}\text{C}$  (Gerothanassis & Tsanaktsidis, 1996; Gerothanassis, 1999; Rehder, 1999). Thus the  $^{17}\text{O}$  nucleus indicates a shielding range  $> 2000$  ppm and  $^{17}\text{O}$  resonances of C-O functional groups indicate a clear-cut distinction between alcohol and ether-type sites and those from C=O groups (Figure 9, Gerothanassis, 1995; Gerothanassis & Kalodimos, 1996; Gerothanassis, 1999).

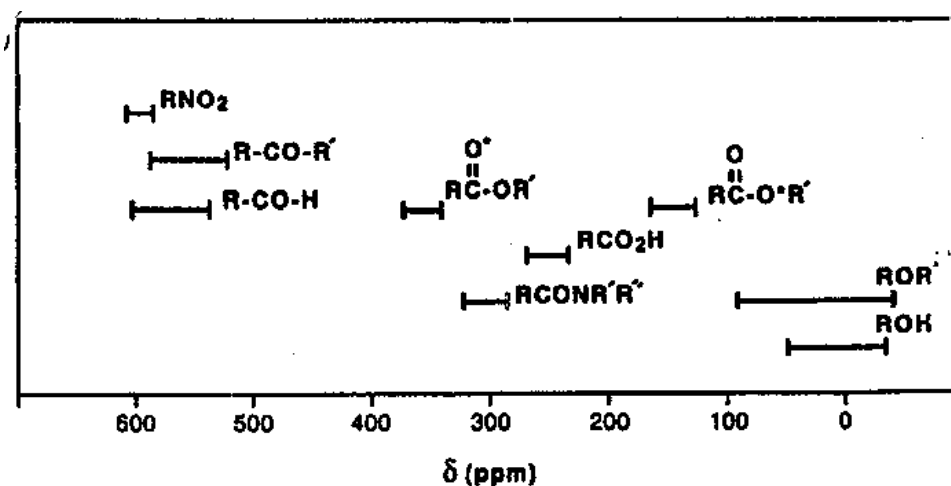


FIGURE 9.  $^{17}\text{O}$  shielding ranges (ppm) for different C-O bonds (Gerothanassis & Kalodimos, 1996).

Transition metal nuclei exhibit even larger shielding ranges. Thus, the  $^{57}\text{Fe}$  nucleus indicates a shielding range  $> 8000$  ppm, which makes it an extremely sensitive probe of electronic and structural investigations (Kalodimos *et al.*, 1999).

## THE FINE STRUCTURE OF THE NMR SPECTRUM

### The coupling constant

When we look, for example, at the  $^1\text{H}$ -NMR spectrum of ethanol (Figure 7), we notice that protons give rise to a triplet and a quartet, each with a rather distinct intensity distribution. The splitting of resonances into individual lines is called the fine structure of the spectrum. It arises because each magnetic nucleus may contribute to the local field experienced by the other nuclei and so modify their resonance frequencies. The strength of the interaction is expressed in terms of the *scalar coupling constant*,  $J$ . Spin coupling constants are independent of the strength of the applied field because they do not depend on the latter's ability to generate local fields. Therefore, they are expressed in hertz (Hz) and not in ppm.

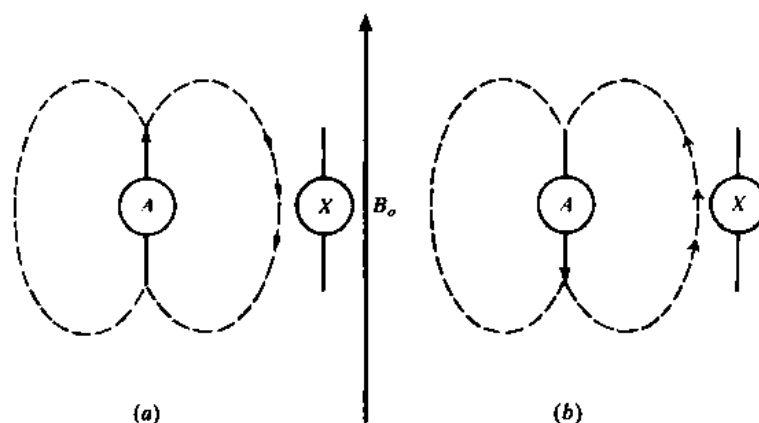


**FIGURE 10.** *The direct coupling of nuclear spins. In (a) the spin of A decreases the net magnetic field at X, while in (b) the field at X is increased (Banwell, 1994).*

Let us consider two hydrogen nuclei, labeled A and X, in different parts of a solid and suppose that are sufficiently close together in space that they exert an appreciable magnetic effect on each other (Figure 10). The lines of force originating from A, considered as a simple bar magnet, are seen to oppose the applied field at X when A is up and to reinforce it when A is down. As the two A directions are virtually equally likely, the X nucleus will find itself in an applied field  $\mathbf{B}_0 + \mathbf{B}_A$  or in  $\mathbf{B}_0 - \mathbf{B}_A$  with equal probability, where  $\mathbf{B}_A$  is the field at X due to nucleus A. This will result in two different resonance conditions for the X nucleus (the X signal will be a doublet in the spectrum) (Banwell, 1994). In general if the resonance line of a particular nucleus is split by a certain amount by a second nucleus, then, the resonance line of the second nucleus is split by the first to the same extent.

This direct, through space, spin-spin interaction or coupling is of practical use in solid-state NMR spectra for measuring interatomic distances with some precision. When liquid or gaseous samples are considered, this direct spin coupling mechanism is found not to apply because random molecular motions within the sample (molecular tumbling) continually change the orientation of the molecules within the applied field and average the coupling exactly to zero. Nonetheless, the NMR spectra of liquids do show the phenomenon of coupling but the effect is very much smaller (by a factor of  $10^2$ - $10^4$  than that observed for direct coupling in solids). It is clear that a different mechanism is involved. Spin-spin coupling in molecules in solution can be explained in terms of a polarization mechanism, in which the interaction of spins is transmitted through the bonds. The magnetic field arising from one nucleus affects the distribution of the electrons in its bond, and the effect can be transmitted through neighboring bonds to other nuclei in the molecule.

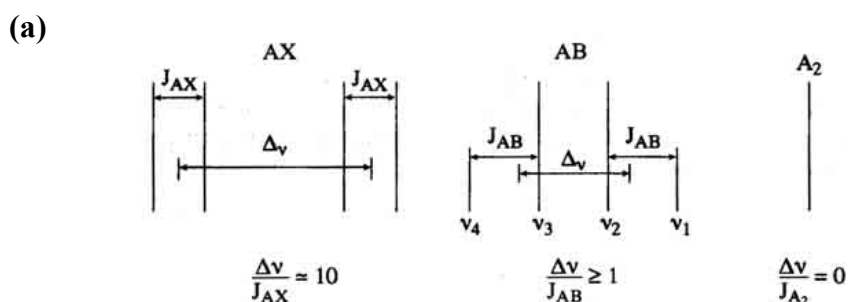
The fact that spin-spin coupling is transmitted through chemical bonds makes the coupling constant,  $J$ , a sensitive parameter for the types of bonds involved and for their spatial orientation in the molecule.

### *Patterns of coupling*

When we have to indicate nuclei with very different chemical shifts, we use letters that are far apart in the alphabet (e.g. A and X). On the contrary, letters close together (e.g. A and B) are used for nuclei with similar chemical shifts. Let us consider a system of A and X nuclei both having spin  $\frac{1}{2}$  and very different chemical shifts, in the sense that the difference in chemical shifts is larger compared to their spin-spin coupling. When the magnetic moment,

$m_I$ , is  $m_I = +\frac{1}{2}$  ( $\uparrow$ ) then we say that we have the  $\alpha$  energy spin state. When  $m_I = -\frac{1}{2}$  ( $\downarrow$ ), then we have the  $\beta$  energy spin state as we can see in Figure 4.

Suppose the spin of X is  $\alpha$ ; then the spin of A will have a Larmor frequency as a result of the combined effect of the external field, the shielding constant and the spin-spin interaction of A with X. The spin-spin coupling will result in one line in the spectrum of A, being shifted by  $-\frac{1}{2}J$  from the frequency it would have in the absence of coupling. Likewise, if the spin of X is  $\beta$ , the spin of A will have a Larmor frequency shifted by  $+\frac{1}{2}J$ . Therefore, instead of a single line from A, we get a doublet of lines separated by  $J$  and centered on the chemical shift characteristic of A (Figure 11(a)) (Atkins, 1998). The same splitting also occurs in the X resonance.



$n = 0$	1
1	1 1
2	1 2 1
3	1 3 3 1
4	1 4 6 4 1
5	1 5 10 10 5 1
6	1 6 15 20 15 6 1

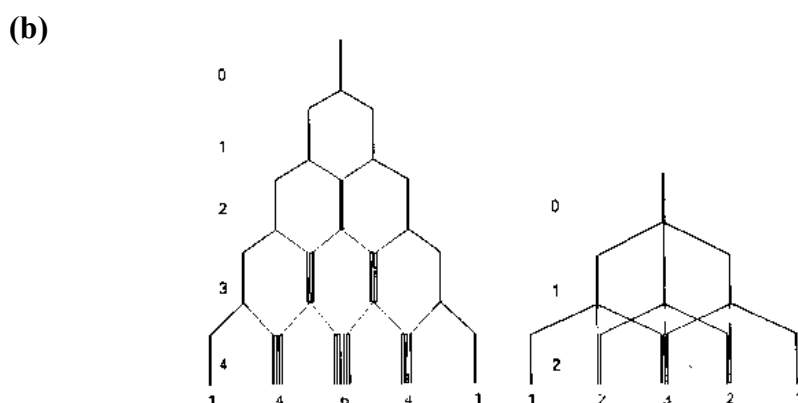


**FIGURE 11.** (a) Dependence of the spectral pattern from the ratio  $\Delta\nu/J$ , (b) Pascal's triangle. The intensity distribution of the A resonance of an  $AX_n$  system can be constructed by considering the splitting caused by 1, 2, ... n nuclei with spin- $\frac{1}{2}$  on the left and spin-1 on the right (Atkins, 1998).

The above analysis refers only to AX systems where  $\Delta\nu / J_{AX} \geq 10$ . In the case of AB systems, where  $10 \gg \Delta\nu \geq J$ , the multiplicity of the peaks remains the same as in AX systems, but the symmetry and the intensity changes significantly. Finally, when the two nuclei have exactly the same chemical shift, then, as a result only one single peak arises in the spectrum (Figure 11(a)).

It is obvious that the peak multiplicity depends on the combination of the interacting spins. In general,  $n$  equivalent spin- $1/2$  nuclei split the resonance of a neighboring spin or group of equivalent spins into  $n+1$  lines with an intensity distribution that obeys Pascal's triangle rule (Figure 11(b)).

We turn now to consider the ethanol spectrum (Figure 7). Consider first the methyl protons. It turns out that the equivalent protons do not show any fine structure. Therefore, an isolated methyl group, as in  $\text{CH}_3\text{Cl}$ , gives a single unsplit line. Next to the methyl group in ethanol are the two methylene protons. The methyl line is first split into two by virtue of the two orientations of one of the two methylene protons, and then each line is split again as a result of the interaction with the second proton. Therefore, the methyl resonance is split into three lines with intensity ratio 1:2:1.

Now consider the splitting of the methylene protons. If they were isolated they would resonate at a single position, as in  $\text{CH}_2\text{Cl}_2$ . Their fine structure is due to their spin-spin interaction with the three neighboring methyl protons. Three equivalent protons give rise to four lines in the intensity ratio 1:3:3:1 (Figure 7).

The hydroxyl proton in ethanol splits its neighbors into two doublets, and it is itself split into a 1:2:1 triplet by the methylene. In practice the splitting due to the hydroxyl proton cannot be detected, as we will explain later.

#### *The magnitudes of coupling constants and their relation to the structure*

The scalar coupling constant of two nuclei separated by  $n$  bonds is denoted as  ${}^nJ$ . As the number of the bonds that separate the two coupled nuclei increases, the interacting energy becomes lower and consequently the coupling constant becomes smaller. Typical values for a proton coupled to a  ${}^{13}\text{C}$  nucleus are:

$$\begin{array}{ll} {}^1J_{\text{CH}} & : \quad 120 - 250 \text{ Hz} \\ {}^2J_{\text{CH}} & : \quad 0 - 10 \text{ Hz} \end{array}$$

On the other hand  ${}^3J$  and  ${}^4J$  give smaller but still detectable effects in a spectrum. Couplings over larger number of bonds ( $n \geq 5$ ) can generally be ignored (Atkins, 1998).

An additional point is that  $J$  varies with the dihedral angle between the bonds (Figure 12). Thus, a  ${}^3J_{\text{HH}}$  coupling constant is often found to depend on the angle  $\varphi$  according to the Karplus equation:

$$J = A + B\cos\varphi + C\cos 2\varphi \quad (11)$$

with A, B, C empirical constants taking values close to + 7 Hz, - 1 Hz, + 5 Hz respectively. Consequently, the measurement of  ${}^3J_{\text{HH}}$  in a series of related compounds can be used to determine their conformations. Additionally, Karplus equation can be used in conformational studies of cyclic systems, steroids, peptides, proteins and other biomolecules (Bovey, 1988):

$${}^3J = 8.5\cos^2\varphi - 0.28 \text{ (Hz)} \quad 0^\circ \leq \varphi \leq 90^\circ \quad (12)$$

$${}^3J = 9.5\cos^2\varphi - 0.28 \text{ (Hz)} \quad 90^\circ \leq \varphi \leq 180^\circ \quad (13)$$

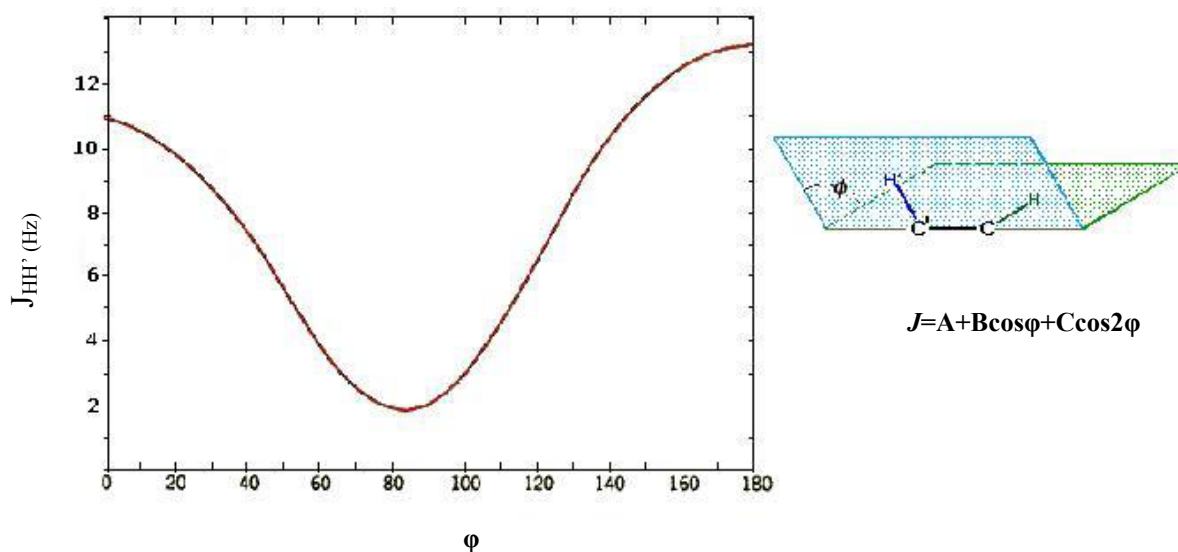


**FIGURE 12.** The variation of the spin-spin coupling constant with angle predicted by the Karplus equation.

It should be emphasized that the low natural abundance of  $^{13}\text{C}$  nucleus provides an advantage:  $^{13}\text{C}$  NMR spectra are easily analyzed as homonuclear  $^{13}\text{C}$ ,  $^{13}\text{C}$  spin-spin coupling constants are absent and the  $^1\text{H}$  NMR spectra of organic molecules are not disturbed by heteronuclear  $^{13}\text{C}$ ,  $^1\text{H}$  coupling. This happens because, in a normal, non-enriched sample,  $^{13}\text{C}$  is present only to the extent of about one per cent natural abundance. So, the probability of two such nuclei being found within a few bonds of each other is very remote. If, for example, there are fewer than 100 carbon atoms in each molecule of the sample, then there will be on average, only one  $^{13}\text{C}$  nucleus per molecule.

### NUCLEAR RELAXATION

Suppose it were possible to drop the NMR sample into the probe instantaneously and then to record the NMR spectrum “immediately”. Would we observe an NMR signal? If we take “immediately” to refer to a period of several seconds, then, the simple answer is yes. At “zero” time, however, the population difference between the lower and upper energy levels would be negligibly small, since the nuclei would experience the very weak Earth’s field. When the field is suddenly changed to the intense field  $\mathbf{B}_0$  of the spectrometer, the process of building up the appropriate Boltzmann population distribution can be quite slow of the order of some seconds. Initially, the nuclear spins are ‘hot’ (essentially equal populations in both states are achieved at infinite temperatures!) and they cool down by transferring some magnetic energy to their surroundings, a process called relaxation.

Once thermal equilibrium has been established, there will be a continuous interchange of spins between the various energy levels, but the overall population ratio will be constant following the statistical Boltzmann equation (5). Application of external radiation at the correct frequency will, however, disturb this population. At resonance, a net absorption will occur because there are more nuclei in the lower energy state. A little thought, however, will reveal that the excess population in the lower level will gradually diminish with time, while the population of the upper level will increase until they become equal; there will then be no net absorption and the signal of a spectrometer designed to detect resonance, will disappear! This phenomenon is known as *saturation* and the NMR experiment would be of little

practical value if it were no means for the spin system to exchange energy with its surroundings. This tends to restore the Boltzmann equilibrium (in opposition to the effects of net absorption of the applied radiofrequency). These restoring processes are known as *relaxation*, and they effectively provide a continuous supply of (excess) nuclei in the lower level of excitation.

When first confronted with nuclear relaxation, the student usually asks: why relaxation is so important in NMR but not in other spectroscopic techniques? Relaxation between rotational or vibrational levels is very effective since the distortion of molecules during collisions often results in changes of rotational and vibrational states. However, relaxation between nuclear spin levels is much slower since changing the orientation of a nucleus is a more difficult task. Consequently, while rotational and vibrational relaxation times are more often of the order of  $10^{-9}$  and  $10^{-4}$  s respectively, relaxation times of seconds are common in NMR (Harris, 1983).

Let us examine the case of a nucleus of  $I = 1/2$ . Transitions between nuclear spin levels can only be induced by magnetic fields. A nucleus in a liquid will experience a fluctuating field, due to the magnetic moments of nuclei in the same or other molecules as they execute Brownian motion. This random fluctuating field may be resolved by Fourier analysis into components oscillating at different frequencies. The component perpendicular to the static field which oscillates with the Larmor frequency, induces transitions between the levels in a similar way to an electromagnetic field. This causes relaxation of both the longitudinal and transverse components of the total magnetization  $M$ . The populations of the states change until they reach the value predicted by the Boltzmann equations for the temperature of the Brownian motion.

It is convenient to consider two different relaxation mechanisms, each of which is effectively a first-order rate process characterized by its own time constant: *spin-lattice* relaxation, of time constant  $T_1$ , occurs because there is exchange of energy between the spin states and the surrounding medium; and *spin-spin* relaxation, of time constant  $T_2$ , occurs with exchange of energy between different nuclear spins. It is useful to think of  $T_1$  processes as affecting the lifetimes of population of spin energy levels, while  $T_2$  processes affect the relative energies of the spin levels rather than lifetimes.

### THE NOE PHENOMENON

The Nuclear Overhauser Effect (NOE) phenomenon provides information about the dipolar interaction, which is the principal mechanism of relaxation for spin-1/2 nuclei. Let us assume that two spins are close enough together that their dipole-dipole interaction is appreciable, or in other words, they are dipole-dipole coupled. The existence of the second spin introduces two more energy levels to the energy level diagram, as shown in Figure 13. By convention the two spins are labeled I and S. The first thing to notice about the energy level diagram in Figure 13, is that there are transitions that involve the simultaneous flip of both spins. These are the transitions  $\alpha\alpha \leftrightarrow \beta\beta$  and  $\alpha\beta \leftrightarrow \beta\alpha$ , with transition probabilities  $W_2$  and  $W_0$  respectively. These two-spins transitions are central to the theory of the NOE, because it is precisely these transitions that give rise to NOE enhancements. Although they are forbidden transitions in the conventional sense, they are not forbidden in the context of relaxation. Both are known as cross-relaxation pathways. The NOE enhancement  $f_1\{S\}$  is defined as the fractional change in the intensity of I on saturating S:

$$f_1\{S\} = (I - I^0) / I^0 \quad (14)$$

where  $I^0$  is the equilibrium intensity of I (Figure 14).

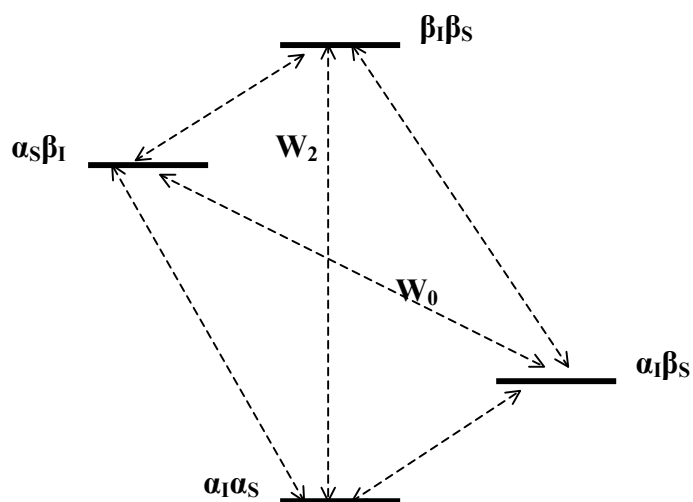


FIGURE 13. Energy level diagram for a two-spin system, I and S, showing definitions of transition probabilities and spin states.

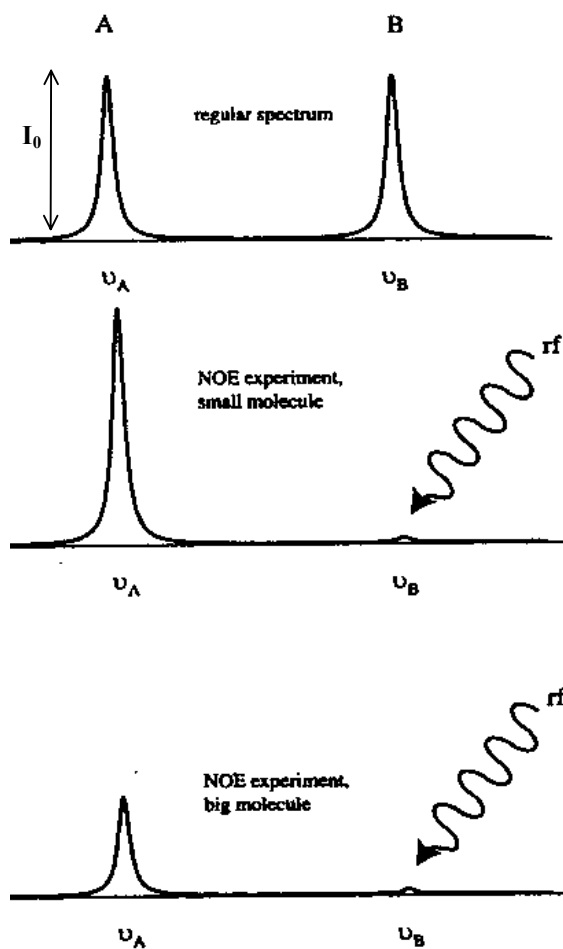


FIGURE 14. The NOE experiment.

When dipole-dipole interaction is present, the z-magnetization of a nucleus I is given by the equation:

$$\frac{dI_z}{dt} = -\rho_I(I_z - I_z^0) - \sigma_{IS}(S_z - S_z^0) \quad (15)$$

where  $\rho_I$  is the relaxation rate of spin I ( $= 1/T_{1(I)}$ ) and  $\sigma_{IS}$  is the cross relaxation rate. From the above equation, we may derive an expression for the steady-state NOE enhancement at I on saturation of S. At steady-state,  $dI_z/dt = 0$  and  $S_z = 0$ , giving  $\rho_I(I_z - I_z^0) = \sigma_{IS}(S_z^0)$ . Thus,  $(I_z - I_z^0) / (S_z^0) = \sigma_{IS} / \rho_I$ . Since,  $S_z^0 = (\gamma_S / \gamma_I) I_z^0$ , we have (Neuhaus & Williamson, 2000; Roberts, 2000):

$$f_1\{S\} = \frac{I_z - I_z^0}{I_z^0} = \frac{\gamma_S}{\gamma_I} \frac{\sigma_{IS}}{\rho_I} \quad (16)$$

Since the dipolar mechanism is a direct through-space interaction with an inverse sixth-power dependence on the internuclear distance of the dipole-dipole coupled nuclei, therefore,  $\text{NOE} \propto 1/r^6$ . This is valid even for the general case of relaxation of a proton by dipolar interaction with many different nuclei. Hence, the observation for instance of an NOE for a certain pair of protons is a good indication that they are located close to one another (within 5 Å) in the molecule, which provides very important structural information.

These studies have recently been extended to much more complicated biological macromolecules such as sugars, nucleotides and proteins (Figure 15). In this last case, NMR can be used in the identification of the aminoacid sequence, as well as in the determination of inter-atomic distances. First, sequence specific resonance assignments of the aminoacids must be obtained for all the protons in the polypeptide chain. Furthermore, each NOE peak can give information that two protons in known locations along the polypeptide chain are separated by a distance of less than 5.0 Å in the three dimensional protein structure. Since the overall length of an extended polypeptide chain with  $n$  residues is  $n \times 3.5$  Å, the NOEs may

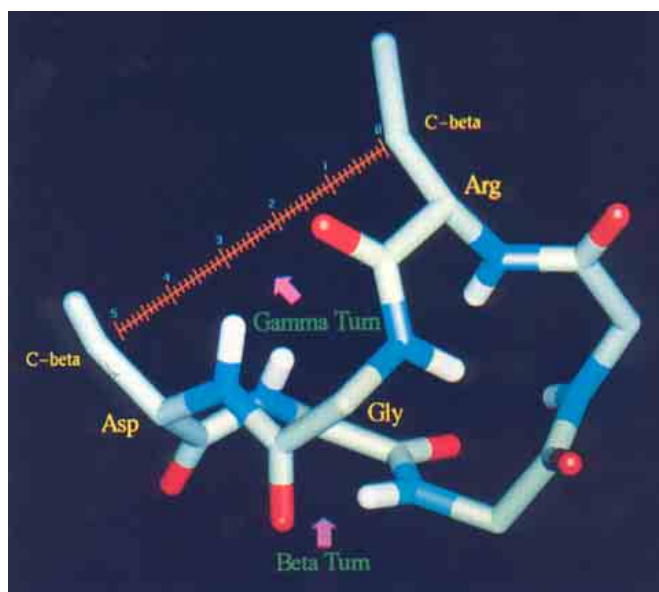


**FIGURE 15.** Fragment of a protein polypeptide chain. NOE is used as a tool for identifying the aminoacid sequence as well as for determining internuclear distances in Å.

impose stringent constraints on the polypeptide conformation. These NOE data, as experimental constraints, can be analyzed in terms of three dimensional arrangements of the polypeptide chain (tertiary structure), by the use of computational techniques (Wüthrich, 1989a; 1989b). Therefore, NMR plays the role of a molecular level camera, where the scale in Figure 15 is expressed in Angstrom ( $\text{\AA}$ ) ( $1 \text{\AA} = 10^{-10} \text{ m}$ ).

## FURTHER APPLICATIONS

### Use of NMR to monitor rate processes

The student may have been puzzled by one aspect of the ethanol spectrum shown in Figure 7. The resonance of the  $-\text{OH}$  hydrogen is shown as a single line whereas we might expect it to be coupled with the neighboring  $\text{CH}_2$  nuclei and hence have multiplet structure. The reason it does not couple is attributed to exchange phenomena. How does it happen?

Let us consider a more general situation in which a nucleus exchanges between two distinct sites, which are designated A and B. An example would be a particular proton on a ligand where the ligand binds to a macromolecule. In this case, the free and bound ligands are apt to have very different chemical shifts. In the limit where no exchange occurs, two distinct resonance lines will be present, one corresponding to each molecular environment. If exchange is extremely rapid, only one line will be evident. Its position will be between the two originally separated lines.

Figure 16 is a schematic representation of the effect of exchange on the spectrum. The

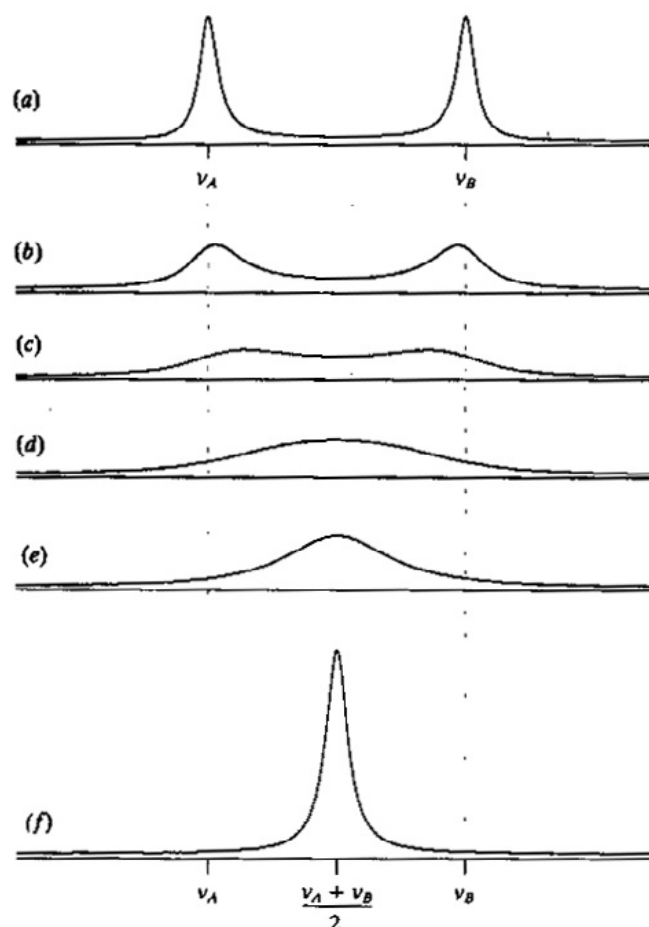


**FIGURE 16.** *The effect of the chemical exchange between two sites A and B on the NMR spectra (Banwell, 1994).*

lifetime in environment A is designated  $\tau_A$ , while  $\tau_B$  denotes the time spent in environment B. The resonance frequencies of the nucleus in the two environments are  $\nu_A$  and  $\nu_B$ . When  $\tau_A \gg (\nu_A - \nu_B)^{-1}$  and  $\tau_B \gg (\nu_A - \nu_B)^{-1}$ , two distinct lines are evident. Under these “slow exchange” conditions, the parameters  $\tau_A$  and  $\tau_B$  can be obtained from a measurement of the increased broadening caused by exchange. When exchange is such that  $\tau_A < (\nu_A - \nu_B)^{-1}$  and  $\tau_B < (\nu_A - \nu_B)^{-1}$ , only a single line width is observed (Figure 16). In this situation, the line width of the coalesced resonance depends on the fractional  $\tau_A$  and  $\tau_B$ . This effect is called exchange broadening.

A similar explanation accounts for the loss of the fine structure of the –OH hydrogen of ethanol (Atkins, 1998). Alcoholic hydroxyl protons are able to exchange with water protons. When this chemical exchange occurs, a molecule ROH with an  $\alpha$ -spin proton ( $\text{ROH}^{(\alpha)}$ ) rapidly turns into  $\text{ROH}^{(\beta)}$  and then into  $\text{ROH}^{(\alpha)}$ , because the protons provided by the solvent molecules in successive exchange have random spin orientations. Therefore, instead of seeing a spectrum composed of contributions from both  $\text{ROH}^{(\alpha)}$  and  $\text{ROH}^{(\beta)}$  molecules (that is a spectrum with lines split into doublets as a result of spin-spin coupling with the hydroxyl proton), all that is seen is a single, unsplit line at the mean position.

### Materials science

NMR spectroscopy, in solid state, can be used to investigate new materials of great technological importance such as glasses, ceramics, polymers, synthetic membranes and superconductors. Furthermore, it can be used to investigate reactions taking place in catalytical surfaces.

### Food chemistry

NMR spectroscopy can be used in the verification of the wine aging and authenticity as well as in the identification of the oil’s fatty constituents (Belton, 1995). It can also

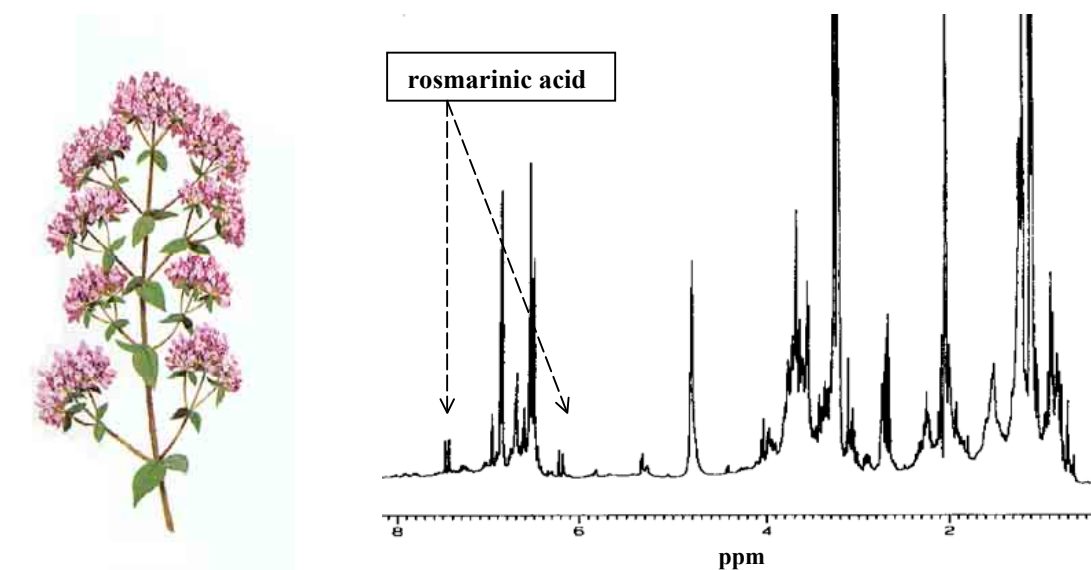


**FIGURE 17.**  $^1\text{H}$ -NMR spectra of the ethanolic extract of the plant *Origanum vulgare* (Greek oregano). The arrows denote the presence of the antioxidant compound rosmarinic acid

contribute in the investigation of the mechanisms that are responsible for food decomposition without the need of sample destruction as it is common with the classical chemical analysis techniques. High resolution NMR techniques have found interesting applications in the analysis of complex mixtures of various extracts of natural products (Gerothanassis, *et al.*, 1998; Exarchou *et al.*, 2001). Figure 17 shows the identification of the antioxidant compound rosmarinic acid in the  $^1\text{H}$  NMR spectra of the ethanolic extract of the plant *Origanum vulgare*. Rosmarinic acid has been reported as a potent active substance against human immunodeficiency virus type one (HIV-1) (Mazumder *et al.*, 1997).

### Clinical applications

NMR has found numerous applications in the localization and characterization of metabolites in biological fluids *in vivo* and *in vitro* and, thus, it can be utilized in the diagnosis of many kinds of diseases. Figure 18, for instance, shows how the rapid screening of urine by NMR spectroscopy can provide information about both the identity of the poison and the resulting abnormal pattern of endogenous metabolites. This pattern is related to the site and severity of toxicity within the kidney, reveals alterations in unusual metabolites that are not commonly measured, and can be used as a noninvasive identification procedure for paraquat poisoning (Bairaktari *et al.*, 1998).

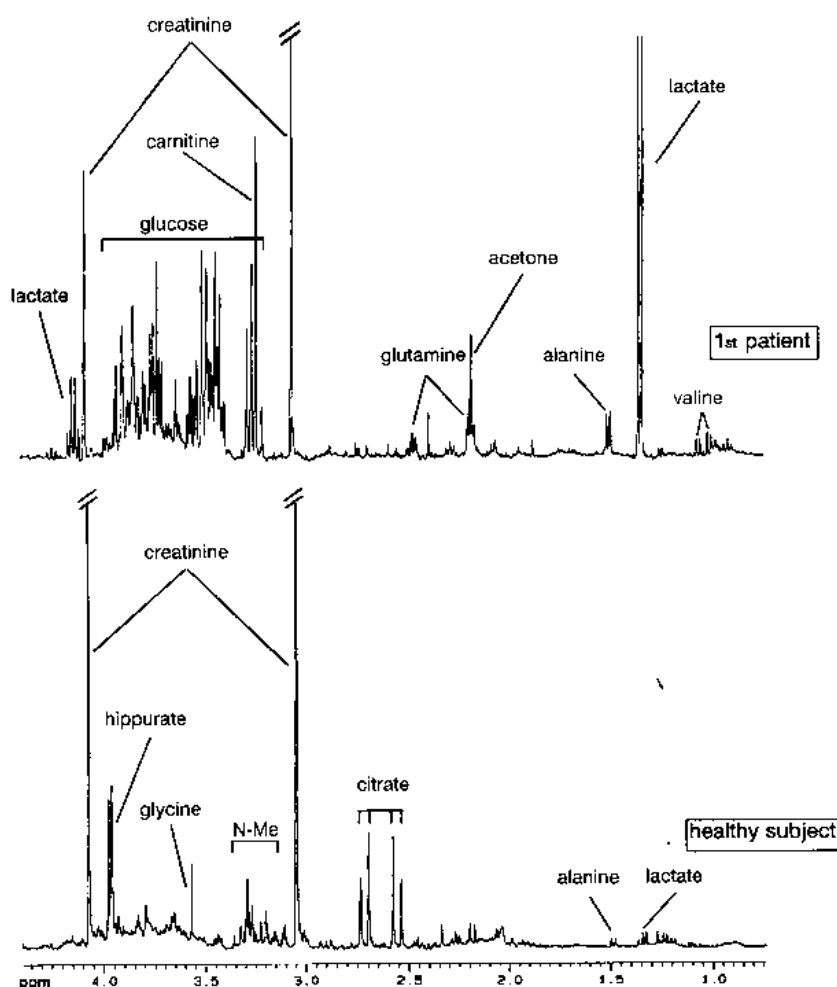


**FIGURE 18.**  $^1\text{H}$ -NMR spectra (400 MHz) of urine from a healthy subject and from one patient suffering from Paraquat intoxication (Bairaktari *et al.*, 1998).

## NMR as a microscope

All the examples mentioned above show that NMR spectroscopy in the hands of chemists, physicists and biologists is perhaps the most powerful tool for studying the matter at a molecular level. A new category of applications is the so-called NMR microscopy or NMR imaging, which is based on the same basic principles as the classical NMR. The difference here is that the signals that are produced vary according to the nuclear density and the properties of the surrounding. Therefore, it is feasible to localize in the three dimensional space the magnetic nuclei (usually protons) allowing the representation of images and the observation of crosscuts of objects with an extraordinary resolution that reaches the millionth of the meter.

NMR microscopy exhibits a variety of technological applications such as the detection of microscopic defects in plastic tubes, the diamond localization in order to avoid breakings during the procedures that follow their excavation. NMR microscopy can also provide valuable information about the fruits' ripening, the best conditions for food handling and even yet about the best cooking temperature conditions, so, unpleasant surprises with frozen fruits returning home after shopping could be avoided! (Figure 19).

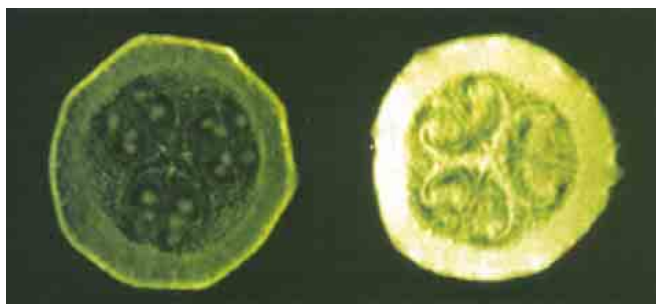


**FIGURE 19.** NMR microscopy of a fresh fruit (on the left) and of a frozen one (on the right).  
Note that the two images were taken without the crosscut of the fruit.

## Magnetic tomography

It was an autumnal morning of the seventies, when several hundreds of demonstrators were gathered in front of a central hospital of an American city protesting against the installation of a bulky instrument with the peculiar name: *Nuclear Magnetic Resonance Tomograph*. Their main demand was to install this “dangerous” instrument away from the center of the city and of any habitable area. Furthermore, the absence of satisfactory security measures (there were only two or three signs, which were forbidding the entrance to those people carrying pacemakers) strengthened the anxiety of the demonstrators. Was this demonstration justified? Has NMR spectroscopy anything to do with the emission of dangerous radiation since it is a “nuclear” phenomenon? The answer is no according to the basic principles, which were outlined above: NMR spectroscopy uses only radiofrequencies. Indeed, the identification of different kind of tissues as well as the visualization of organs' movement consist a very important field of medicare applications, knowing as *magnetic tomography* or *Magnetic Resonance Imaging, MRI*.

Medical community has been very enthusiastic with these new techniques due to many advantages compared to X-rays or to other imaging methods that use radioactive compounds. For instance, the blood volume that is conveyed by the heart in one pulse can be measured, allowing the study of the heart in action. Moreover, soft tissues that it is impossible to be detected using X-rays are clearly shown with the MRI technique, allowing



**FIGURE 20.** *Magnetic Resonance Imaging (MRI): Anatomical view of the brain.*

the diagnosis of tumors and of other diseases. Figure 20 shows a typical application of this technique providing a diagnosis in human brain damages. Recently, investigators claimed that NMR tomography will send very soon the biopsy to retirement. It is well known that during biopsy human tissue is subtracted and the malignancy of a neoplasm is examined under the microscope. On the contrary during the NMR tomography no tissue abstraction is taking place. Instead, a chemical compound with specific properties is infused in human's blood. This compound presents different accumulation in benign tumors in relation to malignant ones. With this methodology, which is completely painless, the insight morphology between, for example, the benign and the malignant breast cancer can be distinguished.

It is obvious that the development of NMR spectroscopy has overcome the most optimistic predictions providing an extremely wide field of impressive applications that are beyond the field of chemistry and are extended to physics, biology, medicine and related disciplines. Therefore, it was not a surprise for the NMR community the recent discovery that NMR can be used for developing quantum computers, with counting speed that reaches million times the speed of the most recent computers. Perhaps it is not a utopia to imagine the time when every personal computer will be connected to its own NMR instrument!

**CORRESPONDENCE:** (a) *Ioannis P. GEROTHANASSIS, Department of Chemistry, Section of Organic Chemistry & Biochemistry, University of Ioannina, Ioannina, GR-45110, Greece; fax: +30 6510 98799; e-mail: igeroth@cc.uoi.gr*

(b) *Anastassios TROGANIS, Department of Biological Applications and Technologies, University of Ioannina, Ioannina, GR-45110, Greece; fax: +30 6510 97064; e-mail: atrogani@cc.uoi.gr*

**Ioannis P. Gerothanassis** is a professor and chairman of the Department of Chemistry, University of Ioannina. He has published over 80 papers, mostly on NMR spectroscopy and its applications to molecules of biological interest.

**Anastassios Troganis** is a lecturer in the Department of Biological Applications and Technologies, University of Ioannina. He has published over 20 papers, including three monographs, mostly on NMR spectroscopy and its applications to molecules of biological interest.

**Vassiliki Exarchou and Klimentini Barbarossou** are Ph.D. students in the Department of Chemistry, University of Ioannina, under Prof. I.P. Gerothanassis' supervision.

## REFERENCES

- Atkins, P.W. (1998). *Physical chemistry* (6<sup>th</sup> edn.). New York: Oxford University Press.
- Bairaktari, E., Katopodis, K., Siamopoulos, K. C., & Tsolas, O. (1998). Paraquat-induced renal injury studied by <sup>1</sup>H-NMR spectroscopy of urine. *Clinical Chemistry*, *44*, 1256-1261.
- Banwell, C.N. (1994). *Fundamentals of molecular spectroscopy* (4<sup>th</sup> edn.). New York: Mc Graw Hill.
- Belton, P.S., Delgadilo, I., Gil, A. M., Webb, G. A., (eds.) (1995). *Magnetic resonance in food science*. Cambridge: The Royal Society of Chemistry.
- Bovey, F.A. (1988). *Nuclear magnetic resonance spectroscopy* (2<sup>nd</sup> edn.). San Diego, California: Academic Press.
- Ernst, R.R., Bodenhausen, A., Wokaun, A. (1987). *Principles of NMR in one and two dimensions*. New York: (Oxford Science Publications), Oxford University Press.
- Exarchou, V., Troganis, A., Gerotheranassis, I.P., Tsimidou, M., & Boskou, D. (2001). Identification and quantification of caffeic and rosmarinic acid in complex plant extracts by the use of variable temperature two dimensional nuclear magnetic resonance spectroscopy. *Journal of Agricultural and Food Chemistry*, *49*, 2-8.
- Gerotheranassis, I.P. (1995). Oxygen-17 NMR. In Grant, D.M. & Harris, R.K. (eds.), *Encyclopedia of nuclear magnetic resonance*, pp. 3430-3440. Chichester: Wiley.
- Gerotheranassis, I.P. (1999). Magnetic resonance: Heteronuclear NMR applications. Oxygen, sulfur, selenium and tellurium magnetic resonance. In Lindon, J.C., Tranter, G.E., & Holmes, J.L. (eds.), *Encyclopedia of spectroscopy and spectrometry*, pp. 722-729. San Diego, California: Academic Press.
- Gerotheranassis, I.P., Exarchou, V., Lagouri, V., Troganis, A., Tsimidou, M., & Boskou, D. (1998). Methodology for identification of phenolic acids in complex phenolic mixtures by high resolution two-dimensional nuclear magnetic resonance. Application to methanolic extracts of two oregano species. *Journal of Agricultural and Food Chemistry*, *46*, 4185-4192.
- Gerotheranassis, I.P. & Kalodimos, C.G. (1996). NMR shielding and the periodic table. *Journal of Chemical Education*, *73*, 801-804.
- Gerotheranassis, I.P. & Tsanaktsidis C.G. (1996). Nuclear electric quadrupole relaxation. *Concepts in Magnetic Resonance*, *8*, 63-74.
- Günther, H. (1995). *NMR spectroscopy - Basic principles, concepts, and applications in chemistry* (2<sup>nd</sup> edn.). Chichester: Wiley.
- Harris, R.K. (1983). *Nuclear magnetic resonance spectroscopy. A physicochemical view*. Massachusetts: Pitman Publishing.
- Hore, P.J. (1995). *Nuclear magnetic resonance*. New York: (Oxford Chemistry Primers, 32), Oxford University Press.
- Kalodimos, C.G., Gerotheranassis, I.P., Rose, E., Hawkes, G.E., & Pierattelli, R. (1999). Iron-57 nuclear shieldings as a quantitative tool for estimating porphyrin ruffling in hexacoordinated carbonmonoxy heme model compounds in solution. *Journal of the American Chemical Society*, *121*, 2903-2908.
- Mazumder, A., Neamati, N., Sunder, S., Schulz, J., Pertz, H., Eich, E., & Pommier, V. (1997). Curcumin analogs with altered potencies against HIV-1 integrase as probes for biochemical mechanisms of drug action. *Journal of Medicinal Chemistry*, *40*, 3057-3063
- McLauchan, K.A. (1972). *Magnetic resonance*. Oxford: (Oxford Chemistry Series), Clarendon Press.
- Neuhaus, D. & Williamson, M.P. (2000). *The Nuclear Overhauser Effect in structural and conformational analysis* (2<sup>nd</sup> edn.). New York: Wiley-VCH.
- Redher, D. (1999). Magnetic resonance: Heteronuclear NMR applications (Sc - Zn). In Lindon, J.C., Tranter, G.E., & Holmes, J.L. (eds.), *Encyclopedia of spectroscopy and spectrometry*, pp. 730-738. San Diego, California: Academic Press.
- Roberts, J.D. (2000). *ABSs of FT-NMR*. Sausalito, California: University Science Books.
- Wüthrich, K. (1989a). The development of nuclear magnetic resonance spectroscopy as a technique for protein structure determination. *Accounts in Chemical Research*, *22*, 36-44.
- Wüthrich, K. (1989b). Protein structure determination in solution by nuclear magnetic resonance spectroscopy. *Science*, *243*, 45-50.